Synthesis of Nanocrystalline Zirconia Using Sol−Gel and Precipitation Techniques

ARTICLE *in* INDUSTRIAL & ENGINEERING CHEMISTRY RESEARCH · NOVEMBER 2006

Impact Factor: 2.59 · DOI: 10.1021/ie060519p

MATERIALS AND INTERFACES

Synthesis of Nanocrystalline Zirconia Using Sol−Gel and Precipitation Techniques

Beena Tyagi,* Kalpesh Sidhpuria, Basha Shaik, and Raksh Vir Jasra*

Silicates and Catalysis Discipline, Central Salt and Marine Chemicals Research Institute (CSMCRI), Bhavnagar 364002, Gujarat, India

Nanocrystalline zirconia samples having predominantly tetragonal crystalline phase were synthesized using sol−gel and conventional precipitation techniques from zirconium hydroxide obtained by the hydrolysis of both zirconium propoxide and zirconium oxychloride precursors. Thermal drying of zirconium hydroxide gel in an oven (110 °C, 12 h) results in lower crystallite size (11−13 nm) as compared to drying under vacuum (50 mbar, 70 °C), which shows higher crystallite size (20−21 nm) during both sol−gel and conventional precipitation synthesis. The progressive transformation of tetragonal to monoclinic phase of zirconia with increasing calcination temperature was observed to be related to the critical crystallite size and lattice strain. Sol−gel synthesis was found to be advantageous because of the stabilization of tetragonal phase at higher temperature, whereas complete phase transformation was observed in the samples prepared by precipitation method at 600−700 °C temperature. Sol−gel synthesis resulted in spherical-shaped particles whereas cubic-/rectangular-shaped particles of varying sizes were predominantly formed by conventional precipitation synthesis.

1. Introduction

Zirconia is an important multifunctional transition metal oxide being widely used in a variety of applications such as ceramics,[1] oxygen[2] and NO*x*[3] sensors, solid oxide fuel cell electrolytes,[4] and semiconductor devices.[5] It has become the ideal media for applications in photonics[6] due to its excellent mechanical, electrical, thermal, optical, and stable photochemical properties. In recent years, zirconia has attracted much attention as a catalyst and catalyst support[7] due to its unique amphoteric character and redox properties. It is reported to catalyze various reactions such as isomerization of alkanes,[8] alkenes,[9] epoxides,[10] and aromatics,[11] dehydration of alcohols,[12] decomposition of nitrous oxide,[13] and selective reduction of citral to geraniol and nerol.[14] It also works as a photocatalyst.[15,16] Reactions such as hydrogenation of olefins,[17] benzene,[18] carbon mono- and dioxide,[19−20] Fischer-Tropsch synthesis,[21] hydrogen production from steam reforming of methanol[22] and ammonia decomposition,[23] low-temperature water−gas shift reaction,[24] and hydrodesulfurization[25] have been reported over zirconia-supported catalysts with higher rates and selectivity than with other supports. Zirconia, after modification with sulfate anions, forms sulfated zirconia that possesses superacidity ($H_0 = -15.9$) and is a potential catalyst for *n*-alkane isomerization at ambient temperature.[26]

Zirconia has three thermodynamically stable crystalline phases under atmospheric pressure: monoclinic (up to 1170 °C), tetragonal (1170−2370 °C), and cubic (2370−2680 °C). However, a metastable tetragonal phase also exists at room temperature that transforms to thermodynamically stable monoclinic phase upon heat treatment. The crystalline phase of zirconia strongly affects its structural, textural, and thereby catalytic properties. For example, zirconia, when stabilized in tetragonal phase as tetragonal zirconia polycrystals (TZP),[27] offers superior strength, toughness, and wear resistance and thus is used in cutting tools, abrasion wheels, etc. Tetragonal phase of zirconia and sulfated zirconia is reported to be catalytically active for many reactions. For example, tetragonal phase of zirconia in Pt/WO_3-ZrO_2 is reported to give higher activity for *n*-butane isomerization[28] and lowers the metallic activity of Pt. Tetragonal phase of sulfated zirconia is known for higher catalytic activity for *n*-butane isomerization[29] and isobutene alkylation[30] compared to monoclinic phase. The crystalline phases of zirconia catalyst can influence a selective reaction and also result in selective products. For example, in CO hydrogenation, methane, ethane, and propene were observed to be the main products with tetragonal zirconia whereas monoclinic zirconia showed higher selectivity for butane.[31] In hydrogenation of olefins, tetragonal zirconia (calcined at 600 °C) showed the maximum activity for 1,3-butadiene, while monoclinic zirconia (calcined at 800 °C) showed the maximum activity for cyclohexadiene.[32] The luminescence properties of Er^{3+}-doped zirconia have also been found to be dependent on the crystalline structure of zirconia.[33] Tetragonal zirconia polycrystals (TZP) are more desirable in arthroplasty[34] due to higher surface hardness and smoothness than monoclinic zirconia ceramic. Therefore, it is very important to have an understanding of the formation of the crystalline phases along with other structural and textural properties of zirconia to tailor it for a particular application.

The formation and transformation of crystalline phases and thereby the catalytic properties of zirconia depend on synthetic parameters such as type of precursor, pH during hydrolysis, doping with ions, and the technique used for its synthesis followed by post-thermal treatments. The influence of various synthetic parameters on the structural and textural properties of zirconia gel have been studied.[35−38]

* To whom correspondence should be addressed. (B. T.) Phone 91-278-2567760 -709. Fax: 91-278-2566970. Email: btyagi@csmcri.org. (R. J.) Phone: 91-278-2471793. Fax: 91-278-2567562. E-mail: rvjasra@csmcri.org.

10.1021/ie060519p CCC: $33.50
Published on Web 11/10/2006

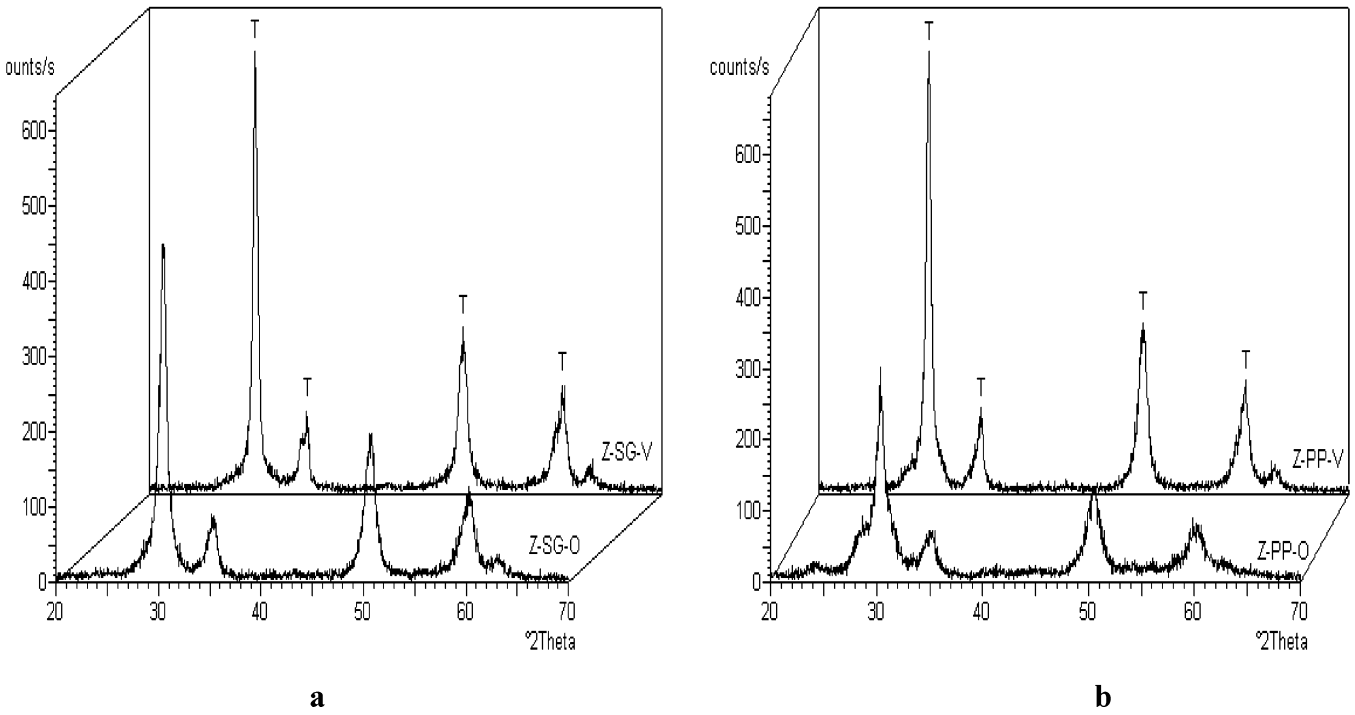

Figure 1. XRD patterns of (a) oven-dried (Z-SG-O) and vacuum-dried (Z-SG-V) sol−gel zirconia samples and (b) oven-dried (Z-PP-O) and vacuum-dried (Z-PP-V) conventional zirconia samples after calcination at 400 °C.

In general, zirconia has been prepared by conventional precipitation method, which is known to give microcrystalline zirconia and also by sol−gel technique to synthesize nanocrystalline zirconia. A nanocrystalline zirconia owing to high surface-to-volume ratio is expected to exhibit enhanced catalytic properties compared to microcrystalline zirconia. The sol−gel technique has been commonly used to prepare metal oxides and is advantageous due to its ease in controlling the purity, homogeneity, and physical characteristics at low temperature.[39−40] Sol−gel followed by supercritical drying of the gel results in aerogels having nanocrystallite size. Recently,[41] we synthesized nanocrystalline mesoporous zirconia using sol−gel followed by supercritical drying, wherein supercritical drying results in smaller crystallite size (4−6 nm) of zirconia as compared to thermally dried zirconia having higher crystallite size (13−20 nm). In the present investigation, we extended our study to compare the thermally dried sol−gel zirconia with thermally dried zirconia prepared by conventional precipitation method using zirconium *n*-propoxide and zirconium oxychloride precursors, respectively. The effect of thermal drying of zirconia gel in an oven and under vacuum has also been studied. The structural and textural properties, namely, crystallite size, crystalline phase, phase transformation with increasing temperature, surface area, and pore volume of zirconia samples prepared by both techniques are determined and compared with a special emphasis on the stabilization of nanocrystalline tetragonal phase and its transformation into nanocrystalline monoclinic zirconia.

2. Experimental Section

2.1. Materials. Zirconium *n*-propoxide, [Zr−P] ($Zr(OC_3H_7)_4$) (70 wt % in *n*-propanol), was procured from Sigma-Aldrich, Germany; zirconium oxychloride ($ZrOCl_2{\cdot}8H_2O$) and *n*-propanol (99%) was obtained from s.d.fine-chem. Ltd., India, and aqueous ammonia solution (25%) was purchased from Rankem, India. All the chemicals were used as such.

2.2. Sol−Gel Synthesis. Seventy weight percent Zr−P diluted to 30 wt % by adding *n*-propanol was used as a zirconia precursor (0.025 M). In a typical experiment, Zr−P (17.7 g) diluted with *n*-propanol (41.3 g) was hydrolyzed by dropwise addition of aqueous ammonia under continuous stirring by magnetic stirrer until the pH of 10−10.5. After the completion of the hydrolysis, the sol was continuously stirred for an hour at ambient temperature to polymerize the gel. The resulting gel was then dried in an oven at a temperature of 110 °C for 12 h as well as under vacuum (50 mbar pressure) at 70 °C temperature in a Rotavapor (BUCHI, R-205). The samples are designated as Z-SG-O and Z-SG-V, respectively.

Scheme 1 . Schematic Representation of the Synthesis of Zirconia by Sol−Gel and Conventional Precipitation Techniques

Sol-gel synthesis:

$$Zr(OC_3H_7)_4 + C_3H_7OH + NH_4OH \xrightarrow{\text{Hydrolysis}} Zr(OH)_4 + C_3H_7OH + NH_3$$
(Zr-*n*-propoxide → Sol)

$$Zr(OH)_4 \xrightarrow{\text{Polycondensation}} [Zr(OH)_4]_n.xC_3H_7OH.xH_2O$$
(Sol → Gel)

$$[Zr(OH)_4]_n.xC_3H_7OH.xH_2O \xrightarrow{110^\circ C} Zr(OH)_4 + C_3H_7OH + H_2O$$
(Amorphous gel)

$$Zr(OH)_4 \xrightarrow{400^\circ C} ZrO_2\ (T) \xrightarrow{500\text{-}700^\circ C} ZrO_2\ (T) + ZrO_2\ (M)$$

Precipitation synthesis:

$$ZrOCl_2.8H_2O + NH_4OH \longrightarrow Zr(OH)_4 + NH_4Cl + H_2O$$
(Zirconium oxychloride → Precipitates)

$$Zr(OH)_4\ (\text{Wet}) \xrightarrow{110^\circ C} Zr(OH)_4\ (\text{Dry}) + H_2O$$

$$Zr(OH)_4 \xrightarrow{400^\circ C} ZrO_2\ (T) \xrightarrow{>400^\circ C} ZrO_2\ (T) + ZrO_2\ (M) \xrightarrow{600\text{-}700^\circ C} ZrO_2\ (M)$$

2.3. Precipitation Synthesis. Eleven grams of $ZrOCl_2{\cdot}8H_2O$ were dissolved in 1400 mL of distilled water (0.025 M) and hydrolyzed by dropwise addition of aqueous ammonia under continuous stirring by magnetic stirrer until the pH of 10−10.5. After hydrolysis, the precipitates were filtered and washed with distilled water until free from chloride ions (checked by $AgNO_3$ solution). The precipitates were then dried in an oven at a

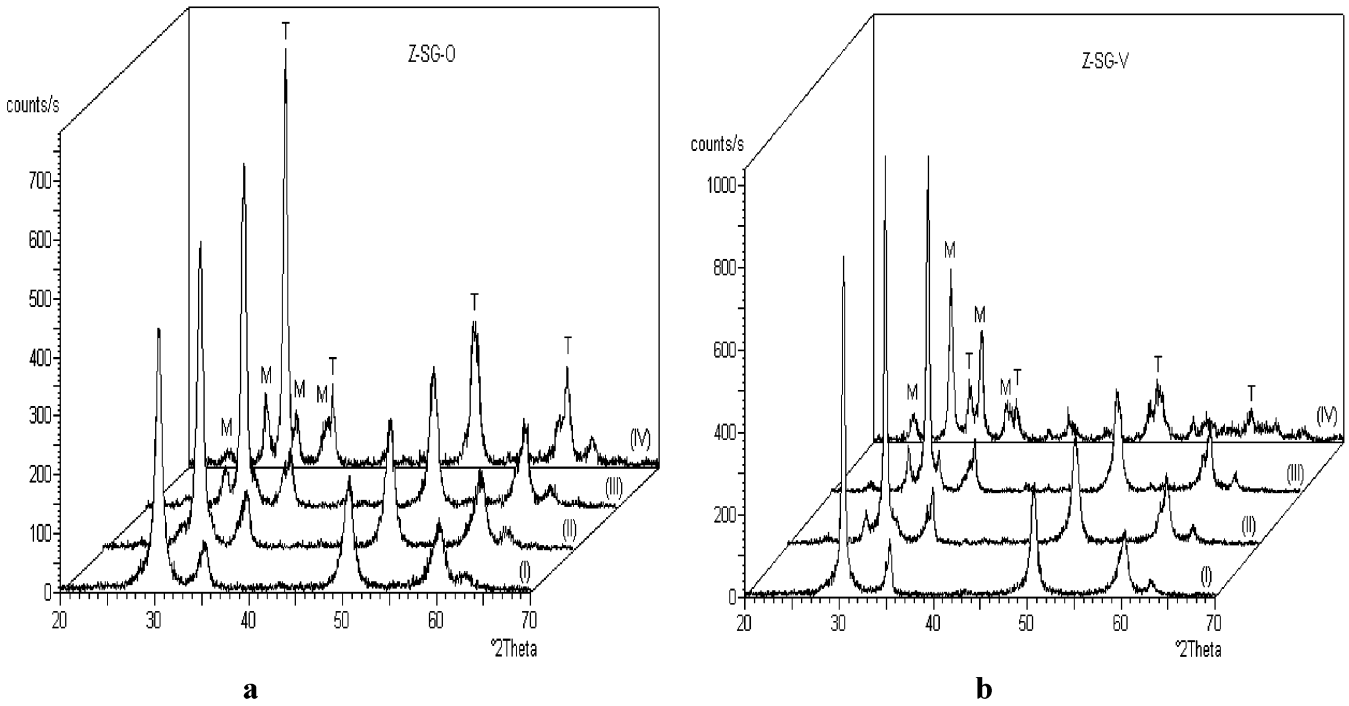

Figure 2. XRD patterns of (a) oven-dried (Z-SG-O) sol−gel zirconia samples after calcination at (I) 400, (II) 500, (III) 600, and (IV) 700 °C and (b) vacuum-dried (Z-SG-V) sol−gel zirconia samples after calcination at (I) 400, (II) 500, (III) 600, and (IV) 700 °C.

Table 1. Crystalline Phases (%) of Oven- and Vacuum-Dried Zirconia Prepared by Sol−Gel and Precipitation Methods at Various Calcination Temperatures[a]

	400 °C		500 °C		600 °C		700 °C	
sample	T	M	T	M	T	M	T	M
Z-SG-O	100		100	-	90	10	80	20
Z-SG-V	100		98	2	84	16	12	88
Z-PP-O	97	3	8	92	1	99		100
Z-PP-V	100		73	27	10	90	4	96

[a] T = tetragonal; M = monoclinic. SG = sol−gel; PP = precipitation; O = oven-dried zirconia; V = vacuum-dried zirconia.

temperature of 110 °C for 12 h as well as under vacuum (50 mbar pressure) at 70 °C temperature in a Rotavapor (BUCHI, R-205). The samples are designated as Z-PP-O and Z-PP-V, respectively.

All the samples prepared were calcined at different temperatures ranging from 400 to 700 °C for 4 h in a static air atmosphere.

2.4. Characterization. 2.4.1. Powder X-ray Diffraction (PXRD). Crystallinity and crystalline phase of zirconia samples formed before and after the calcination at various temperatures were determined with X-ray powder diffractometer (Philips X'pert, MPD system, The Netherlands) using Cu Kα radiation (λ = 1.5405 Å). The samples were scanned in a 2θ range of 0−80° at a scanning rate of 0.4°/s. The crystallite size of the tetragonal (T) and monoclinic (M) phase was calculated from the characteristic peak for tetragonal at 30.5° (111) 2θ angle and monoclinic at 28.4° ($11\bar{1}$) and 31.6° (111) 2θ angle using Scherrer formula:[42]

$$\text{crystalline size} = K\cdot\lambda/W\cdot\cos\theta$$

where K = 0.9, the shape factor, λ = the wavelength of the X-ray used, and $W = (W_b - W_s)$, the difference of the broadened profile width of the experimental sample and the standard width of reference silicon sample.

The quantification[19] of tetragonal and monoclinic phase present in the zirconia was done by comparing the areas of the characteristic peaks of the tetragonal phase (2θ = 30.5° for the (111) reflection) and the monoclinic phase[43] (2θ = 28.4° ($11\bar{1}$), 31.6° (111), 24.2° (011), and 34.1° (002)). The percent composition of each phase was calculated from the net peak area of the characteristic peak determined using software available with the equipment.

$$\%\ \text{tetragonal} = [(\text{peak area})\ \text{tetragonal}/\textstyle\sum (\text{peak area})\ \text{tetragonal and monoclinic}] \times 100$$

$$\%\ \text{monoclinic} = [\textstyle\sum(\text{peak area})\ \text{monoclinic}/\sum (\text{peak area})\ \text{tetragonal and monoclinic}] \times 100$$

2.4.2. FT-IR Spectroscopy. FT-IR spectra of zirconia samples, before and after the calcination, were recorded using a spectrophotometer (Perkin-Elmer Spectrum GX, USA) in the region of 400−4000 cm^{-1} with a resolution of 4 cm^{-1} as KBr pellets having ∼1 wt % of sample.

2.4.3. Thermal Analysis. Thermogravimetric/differential thermal analysis (TG/DTG) of zirconia samples, before calcination, was carried out by Mettler Toledo (TGA/SDTA 861^e, Switzerland) using star^e software. The samples were heated in a temperature range of 50−850 °C at the heating rate of 10 °C min^{-1} under a N_2 atmosphere.

2.4.4. Surface Area, Pore Volume, and Pore Size Distribution. Specific surface area, pore volume, and pore size distributions of zirconia samples, before and after calcination at various temperatures, were determined from nitrogen adsorption−desorption isotherms at 77 K (ASAP 2010, Micromeritics, USA). Surface area and pore volume were determined using BET equation and BJH method,[44] respectively. The samples were degassed under vacuum (5×10^{-3} mmHg) at 120 °C for 4 h, prior to measurement, to evacuate the physiosorbed moisture.

2.4.5. Microscopic Study. The electron microscopic study was done with a scanning electron microscope (Leo series VP1430, Germany) equipped with Oxford Instruments EDX facility, having a silicon detector under a pressure of >1.34 ×

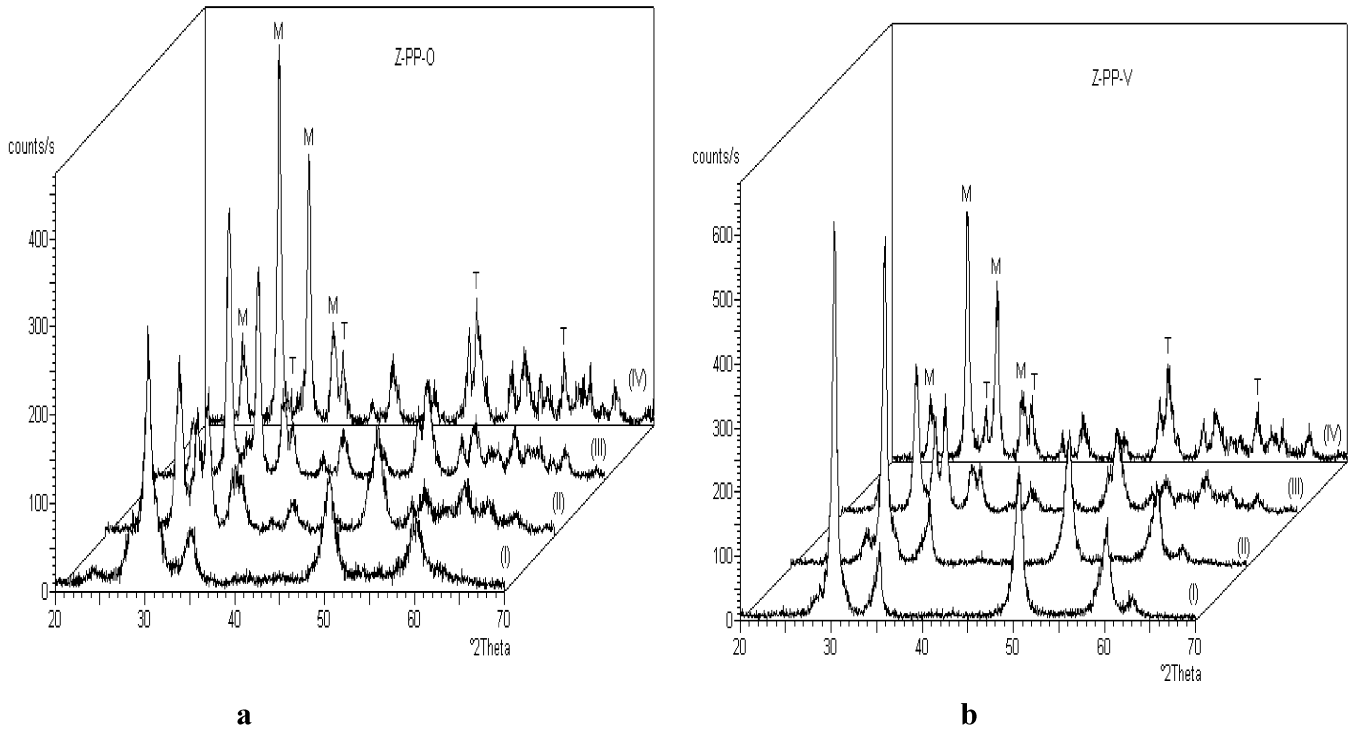

Figure 3. XRD patterns of (a) oven-dried (Z-PP-O) conventional zirconia samples after calcination at (I) 400, (II) 500, (III) 600, and (IV) 700 °C and (b) vacuum-dried (Z-PP-V) conventional zirconia samples after calcination at (I) 400, (II) 500, (III) 600, and (IV) 700 °C.

10^{-2} Pa. The samples were coated with gold using a Polaron Sputter Coater.

3. Results and Discussion

3.1. Structural Properties. 3.1.1. Effect of Thermal Drying. Figure 1a,b shows the PXRD patterns of calcined (400 °C) zirconia samples prepared by sol−gel (SG) and precipitation (PP) methods, respectively, and thermally dried in an oven and under vacuum. All samples were crystalline having predominantly tetragonal (T) phase of zirconia ($2\theta = 30.5°$, 35.3°, 50.7°, 60.4°). In both sol−gel and precipitation methods, zirconium hydroxide is the precursor derived from either zirconium propoxide or zirconium oxychloride as shown in Scheme 1. Formation of tetragonal phase in both SG- and PP-zirconia samples confirms the reported observation[45] that zirconium hydroxide precursor results in tetragonal structure. Samples dried under vacuum showed relatively higher crystallinity as observed by the intensity of characteristic peak of tetragonal phase (counts/s) (Table 2) compared to the oven-dried samples, in both the SG- and PP-zirconia samples.

3.1.2. Effect of Calcination Temperature. Figure 2a,b shows the PXRD patterns of SG-zirconia samples dried in an oven and under vacuum after calcination in the temperature range of 400−700 °C. Calcination at temperatures above 400 °C results in the transformation of tetragonal phase to monoclinic phase of zirconia ($2\theta = 24.2°$, 28.4°, 31.6°, 34.1°) that starts at 500 °C in vacuum-dried zirconia and at 600 °C in oven-dried SG-zirconia samples. Percentage of monoclinic phase was found to be higher (16%) in vacuum-dried zirconia as compared to oven-dried SG-zirconia (10%) at 600 °C; however, after calcination at 700 °C, it sharply increased to 88% as compared to 20% in oven-dried SG-zirconia samples (Table 1).

Formation of monoclinic phase in PP-zirconia samples starts at lower temperature (Figure 3a,b) as compared to that in SG-zirconia samples. For example, Z-PP-O sample was observed to have a small amount (3%) of monoclinic phase along with tetragonal (97%) phase only after calcination at 400 °C (Table 1). Rate of phase transformation was observed to be significantly higher in PP-zirconia samples. For example, PP-zirconia samples were found to have 90−99% monoclinic phase as compared to 10−16% in SG-zirconia samples at 600 °C. A complete (96−100%) transformation of tetragonal to monoclinic phase was observed in PP-zirconia samples after calcination at 700 °C, whereas SG-zirconia samples showed the stabilization of tetragonal phase even at 700 °C (Table 1). These observations clearly show that zirconia prepared by SG-method results in thermally stable tetragonal phase.

3.1.3. Effect on Crystallite Size. Table 2 shows the nanocrystallite size of tetragonal ($2\theta = 30.5°$, (111)) and monoclinic phase ($2\theta = 28.4°$ ($11\bar{1}$) and 31.6° (111)) of SG- and PP-zirconia samples. The samples prepared both by sol−gel and precipitation methods were observed to have nanocrystallite size as also reported by others.[19,46] Among the oven- and vacuum-dried zirconia, crystallite size of oven dried sample was observed to be smaller (11−13 nm) as compared to vacuum-dried sample (20−21 nm) in both SG- and PP-zirconia samples. These observations along with the crystallinity data (peak intensity) of oven- and vacuum-dried samples shown in Figure 1 and Table 2 indicate that the sample showing sharp XRD peaks with higher crystallinity is having higher crystallite size and broadening of XRD peaks along with relative lower crystallinities shows the lower crystallite size.

Crystallite size of both tetragonal and monoclinic phase increases with increasing calcination temperature. The data of Tables 1 and 2 indicate that crystallite size and phase transformation are inter-related. For example, in PP-zirconia samples, crystallite size (11−21 nm) of tetragonal phase ($2\theta = 30.5°$, (111)) starts to increase significantly with the formation of a substantial amount of monoclinic phase and a complete (96−100%) phase transformation occurs when it reaches 32−37 nm. The transformation of crystalline phase of zirconia is reported to depend on various factors such as presence of point defects

Table 2. Crystallinity, Crystallite Sizes, and Lattice Strain of Oven- and Vacuum-Dried Zirconia Prepared by Sol−Gel and Precipitation Methods at Various Calcination Temperatures[a]

			crystallite size, nm (lattice strain)			
sample	phase	peak intensity[b] (counts/s)	400 °C	500 °C	600 °C	700 °C
Z-SG-O	$T_{(111)}$	424	13 (1.201)	14 (1.128)	17 (0.986)	23 (0.769)
Z-SG-V	$T_{(111)}$	721	20 (0.832)	21 (0.816)	23 (0.760)	28 (0.710)
Z-PP-O	$T_{(111)}$	257	11 (1.415)	15 (1.110)	32 (0.587)	
	$M_{(11\bar{1})}$			11 (1.509)	17 (1.061)	26 (0.736)
	$M_{(111)}$			16 (0.978)	20 (0.817)	30 (0.597)
Z-PP-V	$T_{(111)}$	471	21 (0.816)	22 (0.773)	29 (0.629)	37 (0.525)
	$M_{(11\bar{1})}$				16 (1.081)	29 (0.681)
	$M_{(111)}$				19 (0.831)	25 (0.692)

[a] T = tetragonal; M = monoclinic; SG = sol−gel; PP = precipitation; O = oven-dried zirconia; V = vacuum-dried zirconia. [b] Crystallinity in terms of peak intensity of $T_{(111)}$ phase of zirconia samples after calcination at 400 °C.

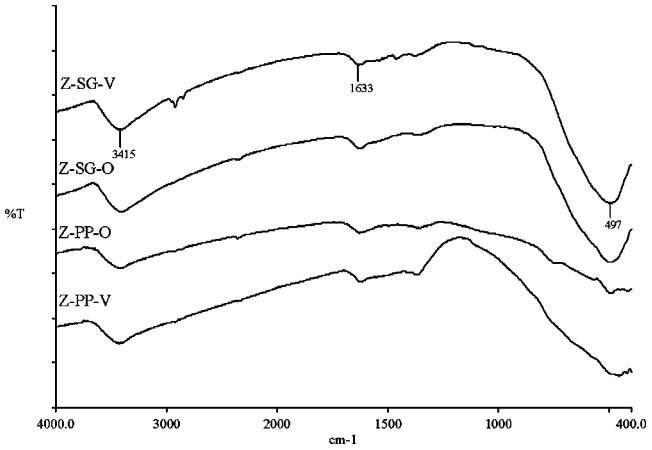

Figure 4. FT-IR spectra of the zirconia samples after calcination at 400 °C.

generated during dehydroxylation,[47] presence of water vapor facilitating the transformation at lower temperature,[48] large particles transformation at a lower temperature than small particles,[49] and rapid transformation at room temperature by grinding or ultrasonic treatment[50] at 400 kHz. Ceramic tetragonal zirconia polycrystals (TZP) used as implanted femoral heads reported to undergo phase transformation of the surface layers with increasing time of implantation.[34] Our results were found

Table 3. Textural Properties of Oven- and Vacuum-Dried Zirconia Prepared by Sol−Gel and Precipitation Methods before and after Calcination at 400 °C[a]

sample	before and after calcination (°C)	BET (m^2/g)	pore volume (cm^3/g)	pore diameter (Å)	micropore volume (cm^3/g)
Z-SG-O	before	177	0.119	26	0.020
	400	100	0.080	32	
Z-SG-V	before	210	0.138	26	0.065
	400	44	0.046	42	
Z-PP-O	before	327	0.183	22	0.013
	400	149	0.130	35	
Z-PP-V	before	233	0.127	22	0.035
	400	92	0.088	38	

[a] SG = sol−gel; PP = precipitation; O = oven-dried zirconia; V = vacuum-dried zirconia.

in accordance with Garvie,[51] who reported that during calcination at increasing temperature, initially, a trace amount of monoclinic phase is observed because some of the crystallite had a size greater than a critical value and at higher temperature all the crystallites exceeded the critical value so that the entire sample transforms to monoclinic phase. Garvie[51] further showed the critical crystallite size of tetragonal phase of zirconia to be 30 nm before complete phase transformation occurs. In the present study, we also observed crystallite size of 32−37 nm for complete transformation from tetragonal to monoclinic phase (at 600−700 °C) in PP-zirconia samples. In SG-zirconia sample,

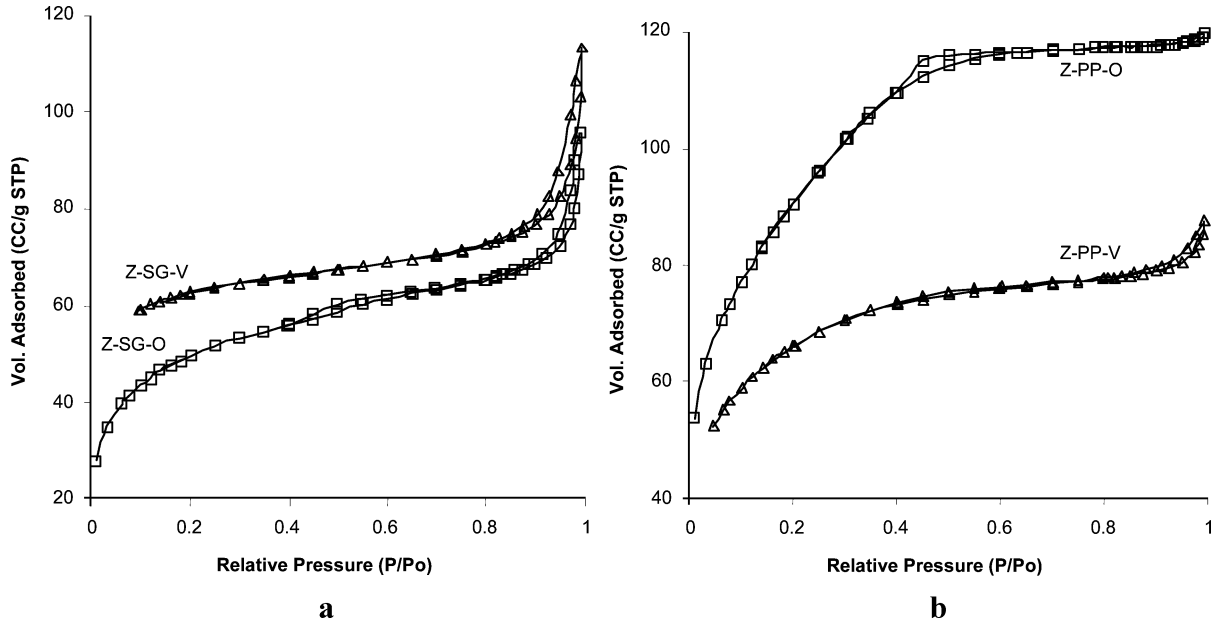

Figure 5. N_2 adsorption−desorption isotherms of (a) oven-dried (Z-SG-O) and vacuum-dried (Z-SG-V) sol−gel zirconia samples and (b) oven-dried (Z-PP-O) and vacuum-dried (Z-PP-V) conventional zirconia samples before calcination.

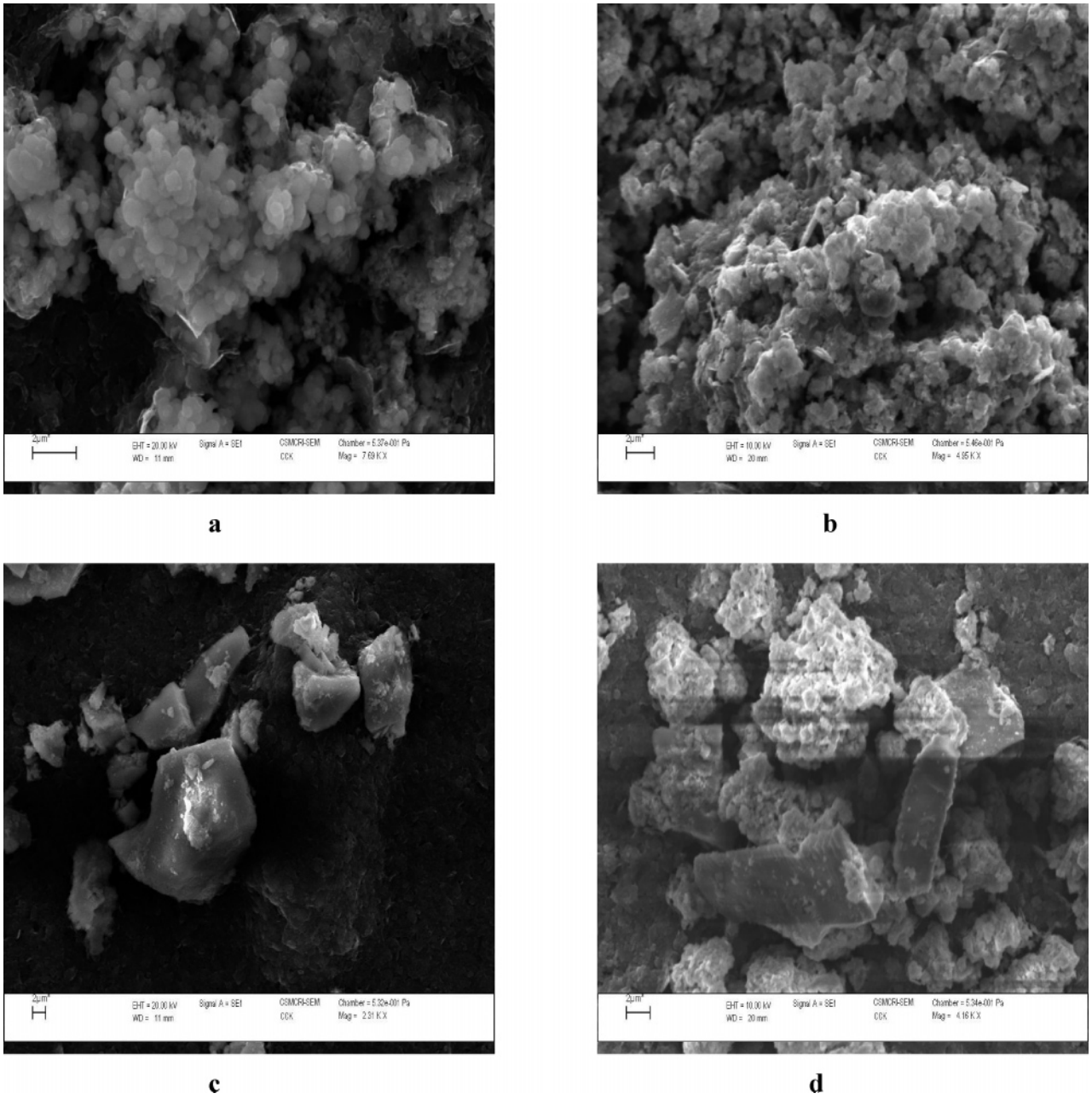

Figure 6. SEM images of (a) oven-dried (Z-SG-O) and (b) vacuum-dried (Z-SG-V) sol−gel zirconia samples and (c) oven-dried (Z-PP-O) and (d) vacuum-dried (Z-PP-V) conventional zirconia samples before calcination.

crystallite size (23−28 nm) does not exceed the critical size until 700 °C, reflecting the stabilization of tetragonal phase; however, larger size (28 nm) of SG-V sample could be responsible for a sharp increase in monoclinic phase (88%) as compared to SG-O sample which has lower crystallite size (20 nm) and showed only 20% monoclinic phase at 700 °C. In our previous work[52] also the crystallite size of zirconia, prepared by the sol−gel method, was found to increase from 13 to 23 nm having 29% monoclinic phase at 600 °C. Crystallite size of monoclinic (28.4° ($11\bar{1}$) and 31.6° (111)) was also found to be 25−30 nm in samples having predominantly (96−100%) monoclinic phase.

The critical crystallite size of tetragonal phase strongly depends on internal stresses at any given temperature. With correlation of the crystallite size with lattice strain obtained from XRD data (Table 2), it was observed that (i) the smaller the crystallite size, the higher the lattice strain and (ii) lattice strain in both tetragonal and monoclinic crystallites decreases with increasing calcination temperature. Therefore, during calcination at higher temperature, lattice strain decreases, resulting in the increase in crystallite size. Lattice strain of Z-PP-O (1.415) and Z-PP-V (0.816) samples having tetragonal crystallites of 11−21 nm decreased to 0.587 and 0.525, respectively, having tetragonal crystallite size of 32−37 nm at 600−700 °C, which is the critical tetragonal crystallite size and the samples completely (96−100%) transformed to monoclinic crystallites. Lattice strain of tetragonal crystallites in SG-zirconia samples was observed to be higher as compared to PP-zirconia at a given temperature and, therefore, samples have not exceeded the critical crystallite size. Furthermore, within the monoclinic phase, crystallite size of 28.4° 2θ ($11\bar{1}$) was observed to have higher lattice strain than 31.6° 2θ (111) and hence showed smaller crystallite size at a given temperature.

However, the crystallite size is not solely responsible for phase transformation. In the present study, we have observed the crystallite sizes of both SG- and PP-zirconia samples were

found in a similar range; for example, oven-dried SG- and PP-zirconia were in the range of 11−13 nm and vacuum-dried in the range of 20−21 nm. However, in SG-zirconia samples tetragonal phase was found to be stable at higher temperature as compared to PP-zirconia samples. It could be explained in terms of the presence of homogeneously distributed and higher number of chemically bound hydroxyl groups in sol−gel synthesis as reported by Gomez and Lopez[47] that stabilization of tetragonal phase in sol−gel zirconia occurs in a different way than conventional precipitation; in the latter technique large ions such as Y, Ce, Ca, or Mg are required to dope it, whereas in the sol−gel technique the hydroxide ions stabilize the tetragonal phase and which upon dehydroxylation transform into monoclinic zirconia.

3.2. FT-IR Spectroscopic Studies. Figure 4 shows the FT-IR spectra of zirconia samples calcined at 400 °C. The band at 490−501 cm^{-1} is attributed to Zr−O−Zr bond. The samples prepared by the sol−gel method show the sharp band in the Zr−O−Zr region, indicating the significant affect of synthesis procedure on the bonding of zirconia. The presence of adsorbed water molecule in zirconia samples is shown by the bands at around 3400 and 1630 cm^{-1} as stretching and bending frequencies, respectively.

3.3. Thermogravimetric Analysis. TG/DTG profile of both SG- and PP-zirconia samples showed the maximum weight loss in the range of 22−33%.

3.4. Textural Properties. Table 3 shows the textural properties of SG- and PP-zirconia samples as such and after calcination at 400 °C. Initially, the samples were found to have BET surface area in the range of 177−327 $m^2\ g^{-1}$, which decreased after calcination at 400 °C. PP-zirconia samples have been observed to have higher surface area (233−327 $m^2\ g^{-1}$) as compared to SG-zirconia samples (177−210 $m^2\ g^{-1}$). The micropore volume calculated from t-plot data showed that vacuum-dried samples possess higher micropore volume as compared to oven-dried samples in both SG- and PP-zirconia samples. The higher rate of decrease in surface area observed in vacuum-dried samples in both SG-zirconia (79%) and PP-zirconia (61%) as compared to oven-dried samples of SG-zirconia (44%) and PP-zirconia (54%) after calcination at 400 °C is due to the presence of higher microporosity in vacuum-dried samples which collapse upon calcination. Similarly, the rate of decrease in pore volume after calcination at 400 °C was also observed to be higher in vacuum-dried samples in both SG-zirconia (67%) and PP-zirconia (31%) than oven-dried samples of SG-zirconia (33%) and PP-zirconia (29%). However, the average pore diameter of all the samples from both SG- and PP-zirconia was found to be in the range of 22−26 Å, which increased to 32−42 Å after calcination at 400 °C. Figure 5 shows the N_2 adsorption−desorption isotherm of SG- and PP-zirconia samples dried in an oven and under vacuum before calcination. Both the samples showed not well-defined type of isotherm as per IUPAC; however, the shape of isotherms shows the presence of micropores, mesopores, and macropores. The presence of both H3 and H2 hysteresis indicates the combined presence of ink-bottle and slit-shaped pores[43] in these samples.

3.4. Microscopic Properties. The surface morphology of the zirconia samples prepared by sol−gel and precipitation methods was found to be different. The samples prepared by sol−gel were observed to have spherical-shaped particles thermally dried by either oven or vacuum (Figure 6a,b), whereas samples prepared by precipitation method were found to have predominantly cubic-/rectangular-shaped particles of varying sizes in oven-dried samples (Figure 6c) along with some spherical particles in vacuum-dried samples (Figure 6d).

Conclusions

Nanocrystalline zirconia having predominantly tetragonal crystalline phase can be synthesized by sol−gel as well as conventional precipitation techniques from zirconium hydroxide obtained by the hydrolysis of both zirconium propoxide and zirconium oxychloride precursors. Thermal drying of zirconium hydroxide gel significantly affects the crystallite size of zirconia. Drying in an oven (110 °C, 12 h) results in lower crystallite size (11−13 nm) as compared to drying under vacuum (50 mbar, 70 °C), which results in higher crystallite size (20−21 nm) in both sol−gel and conventional precipitation synthesis. The progressive transformation of tetragonal to monoclinic phase occurs with increasing calcination temperature accompanied by the increase of crystallite size. Phase transformation was observed to be related to the critical crystallite size and lattice strain. Sol−gel synthesis showed the stabilization of tetragonal phase at higher temperature, whereas complete phase transformation was observed in the samples prepared by precipitation method. Sol−gel samples were observed to have spherical-shaped particles, whereas conventional samples were of irregular rectangular-shaped particles of varied size. Both the techniques result in nanocrystalline zirconia; however, the sol−gel technique is advantageous particularly to prepare stabilized nanocrystalline tetragonal zirconia.

Acknowledgment

Authors are thankful to Dr. P. K. Ghosh, Director, CSMCRI, for his encouragement. We are also thankful to Dr. (Mrs.) P. A. Bhatt, Mr. V. B. Boricha and Mr. Chandrakanth C. K. for X-ray, FT-IR and SEM analysis support.

Literature Cited

(1) Jin, X. J. Martensitic Transformation in Zirconia Containing Ceramics and Its Applications. *Curr. Opin. Solid State Mater. Sci.* **2006**, in press.

(2) Zhou, M.; Ahmad, A. Synthesis, Processing and Characterization of Calcia-Stabilized Zirconia Solid Electrolytes for Oxygen Sensing Applications. *Mater. Res. Bull.* **2006**, *41*, 690.

(3) Zhuiykov, S.; Miura, N. Development of Zirconia-based Potentiometric NO_x Sensors for Automotive and Energy Industries in the early 21st Century: What are the Prospects for Sensors? *Sens. Actuators, B* **2006**, in press.

(4) Fergus, J. W. Electrolytes for Solid Oxide Fuel Cells. *J. Power Sources* **2006**, *162*, 30.

(5) Wilk, G. D.; Wallace, R. M. Stable Zirconium Silicate Gate Dielectrics Deposited Directly on Silicon. *Appl. Phys. Lett.* **2000**, *76*, 112.

(6) Rosa-Cruz, E. De la.; Diaz-Torres, L. A.; Salas, P.; Castano, V. M.; Hernandez, J. M. Evidence of Non-Radiative Energy Transfer from the Host to the Active Ions in Monoclinic ZrO_2: Sm^{+3}. *J. Phys. D: Appl. Phys.* **2001**, *34*, 83.

(7) Corma, A. Inorganic Solid Acids and Their Use in Acid-Catalyzed Hydrocarbon Reactions. *Chem. Rev.* **1995**, *95*, 559.

(8) Vartuli, J. C.; Santiesteban, J. G.; Traverso, P.; Cardona-Martinez, N.; Chang, C. D.; Stevenson, S. A. Characterization of the Acid Properties of Tungsten/Zirconia Catalysts Using Adsorption Microcalorimetry and n-Pentane Isomerization Activity. *J. Catal.* **1999**, *187*, 131.

(9) Nakano, Y.; Iizuka, T.; Hattori, H.; Tanabe, K. Surface Properties of Zirconium Oxide and its Catalytic Activity for Isomerization of 1-Butene. *J. Catal.* **1979**, *57*, 1.

(10) Arata, K.; Akutagawa, S.; Tanabe, K. Epoxide Rearrangement III. Isomerization of 1-Methylcyclohexene Oxide over TiO_2-ZrO_2, $NiSO_4$ and $FeSO_4$. *Bull. Chem. Soc. Jpn.* **1976**, *49*, 390.

(11) Wilson, R. D.; Barton, D. G.; Baertsch, C. D.; Iglesia, E. Reaction and Deactivation Pathways in Xylene Isomerization on Zirconia Modified by Tungsten Oxide. *J. Catal.* **2000**, *194*, 175.

(12) Ferino, I.; Casula, M. F.; Corrias, A.; Cutrufello, M. G.; Monaci, R.; Paschina, G. 4-Methylpentan-2-ol Dehydration over Zirconia Catalysts Prepared by Sol−Gel. *Phys. Chem. Chem. Phys.* **2000**, *2*, 1847.

(13) Miller, T. M.; Grassian, V. H. Environmental Catalysis: Adsorption and Decomposition of Nitrous Oxide on Zirconia. *J. Am. Chem. Soc.* **1995**, *117*, 10969.

(14) Zhu, Y.; Liu, S.; Jaenicke, S.; Chuah, G. Zirconia Catalysts in Meerwein-Ponndrof-Verley Reduction of Citral. *Catal. Today* **2004**, *97*, 249.

(15) Kohno, Y.; Tanaka, T.; Funnabiki, T.; Yoshida, S. Identification and Reactivity of a Surface Intermediate in the Photoreduction of CO_2 with H_2 over ZrO_2. *J. Chem. Soc., Faraday Trans.* **1998**, *94*, 1875.

(16) Navio, J. A.; Colon, G.; Herrmann, J. M. Photoconductive and Photocatalytic Properties of $ZrTiO_4$. Comparison with the Parent Oxides TiO_2 and ZrO_2. *J. Photochem. Photobiol. A: Chem.* **1997**, *108*, 179.

(17) D'Souza L.; Suchopar, A.; Zhu, K.; Balyozova, D.; Devadas, M.; Richards, R. M. Preparation of Thermally Stable High Surface Area Mesoporous Tetragonal ZrO_2 and Pt/ZrO_2: An Active Hydrogenation Catalyst. *Microporous Mesoporous Mater.* **2006**, *88*, 22.

(18) Arribas, M. A.; Marquez, F.; Martinez, A. Activity, Selectivity and Sulfur Resistance of Pt/WO_x-ZrO_2 and Pt/Beta Catalysts for the Simultaneous Hydroisomerization of n-Heptane and Hydrogenation of Benzene. *J. Catal.* **2000**, *190*, 309.

(19) Su, C.; Li, J.; He, D.; Cheng, Z.; Zhu, Q. Synthesis of Isobutene from Synthesis gas over Nanosize Zirconia Catalysts. *Appl. Catal., A* **2000**, *202*, 81.

(20) Jung, K. T.; Bell, A. T. Effects of Zirconia Phase on the Synthesis of Methanol over Zirconia-Supported Copper. *Catal. Lett.* **2002**, *80*, 63.

(21) Zhou, Z.; Zhang, Y.; Tierney, J. W.; Wender, I. Hybrid Zirconia Catalysts for Conversion of Fischer−Tropsch Waxy Products to Transportation Fuels. *Fuel Process. Technol.* **2003**, *83*, 67.

(22) Yao, C. Z.; Wang, L. C.; Liu, Y. M.; Wu, G. S.; Cao, Y.; Dai, W. L.; He, H. Y.; Fan. K. N. Effect of Preparation Method on the Hydrogen Production from Methanol Steam Reforming Over Binary Cu/ZrO_2 Catalysts. *Appl. Catal., A* **2006**, *297*, 151.

(23) Yin, S. F.; Xu, B. Q.; Wang, S. J.; Au, C. T. Nanosized Ru on High-Surface-Area Superbasic ZrO_2−KOH for Efficient Generation of Hydrogen via Ammonia Decomposition. *Appl. Catal., A* **2006**, *301*, 202.

(24) Lida, H.; Igarashi, A. Structure Characterization of $Pt-Re/TiO_2$ (rutile) and $Pt-Re/ZrO_2$ Catalysts for Water Gas Shift Reaction at Low-Temperature. *Appl. Catal., A* **2006**, *303*, 192.

(25) Li, G.; Li, W.; Zhang, M.; Tao, K. Morphology and Hydrodesulfurization Activity of CoMo Sulfide Supported on Amorphous ZrO_2 Nanoparticles Combined with Al_2O_3. *Appl. Catal., A* **2004**, *273*, 233.

(26) Hino, M.; Arata, K. Synthesis of Solid Acid Catalysts with Acid Strength of H_o>-16.04. *J. Chem. Soc., Chem. Commun.* **1980**, 851.

(27) Wattanasiriwech, D.; Wattanasiriwech, S.; Stevens, R. A Sol-Powder Coating Technique for Fabrication of Yttria Stabilised Zirconia. *Mater. Res. Bull.* **2006**, *41*, 1437.

(28) Yori, J. C.; Parera, J. M. Influence of the Crystalline Structure of ZrO_2 on the Metallic Properties of Pt/WO_3-ZrO_2. *Catal. Lett.* **2000**, *65*, 205.

(29) Stichert, W.; Schuth, F.; Kuba, S.; Knozinger, H. Monoclinic and Tetragonal High Surface Area Sulfated Zirconias in Butane Isomerization: CO Adsorption and Catalytic Results. *J. Catal.* **2001**, *198*, 277.

(30) Zalewski, D. J.; Alerasool, S.; Doolin, P. K. Characterization of Catalytically Active Sulfated Zirconia. *Catal. Today* **1999**, *53*, 419.

(31) Li, W.; Yin, Y.; Gao, R.; Hou, R. Comparison of Co Hydrogenation on Monoclinic and Tetragonal ZrO_2 Catalysts. *Fenzi Cuihua (China)* **1999**, *13*, 186.

(32) Tanabe, K. Surface and Catalytic Properties of ZrO_2. *Mater. Chem. Phys.* **1985**, *13*, 347.

(33) Santos, E. M.; Vohra S.; Catledge, S. A.; McClenny, M. D.; Lemons, J.; David Moore, K. Examination of Surface and Material Properties of Explanted Zirconia Femoral Heads. *J. Arthroplasty* **2004**, *19*, 30.

(34) Patra, A. Effect of Crystal Structure and Concentration on Luminescence in Er^{+3}: ZrO_2 Nanocrystals. *Chem. Phys. Lett.* **2004**, *387*, 35.

(35) Livage, J.; Sanchez, C. Sol−Gel Chemistry. *J. Non-Cryst. Solids* **1992**, *145*, 11.

(36) Pan, M.; Liu, J. R.; Lu, M. K.; Xu, D.; Yuan, D. R.; Chen, D. R.; Yang, P.; Yang, Z. H. Preparation of Zirconia Xerogels and Ceramics by Sol−Gel Method and the Analysis of Their Thermal Behavior. *Thermochim. Acta* **2001**, *376*, 77.

(37) Kongwudthiti, S.; Praserthdam, P.; Silveston, P.; Inoue, M. Influence of Synthesis Conditions on the Preparation of Zirconia Powder by the Glycothermal Method. *Ceram. Int.* **2003**, *29*, 807.

(38) Jiao, X.; Chen, D.; Xiao, L. Effects of Organic Additives on Hydrothermal Zirconia Nanocrystallites. *J. Cryst. Growth* **2003**, *258*, 158.

(39) Celzard, A.; Mareche, J. F. Application of the Sol−Gel Process Using Well-Tested Recipes. *J. Chem. Educ.* **2002**, *79*, 854.

(40) Ward, D. A.; Ko, E. I. Preparing Catalytic Materials by the Sol−Gel Method. *Ind. Eng. Chem. Res.* **1995**, *34*, 421.

(41) Tyagi, B.; Sidhpuria, K.; Shaik, B.; Jasra, R. V. Synthesis and Characterization of Nano-crystalline Mesoporous Zirconia Using Supercritical Drying. *J. Nanosci. Nanotechnol.* **2006**, *6*, 1584.

(42) Cullity, B. D.; Stock, S. R. *Elements of X-ray Diffraction*, 3rd ed.; Prentice Hall: Upper Saddle River, NJ, 2001; p 388.

(43) 13-0307, JCPDS-ICDD copyright, Sets 1−46 database, 1996.

(44) Gregg, S. J.; Sing, K. S. W. *Adsorption, Surface Area and Porosity*, 2nd ed.; Academic Press: New York, 1982.

(45) Torralvo, M. J.; Alario, M. A.; Soria, J. Crystallization Behavior of Zirconium Oxide Gels. *J. Catal.* **1984**, *86*, 473

(46) Wang, J. A.; Valenzuela, M. A.; Salmones, J.; Vazquez, A.; Garcia-Ruiz, A.; Bokhimi, X. Comparative Study of Nanocrystalline Zirconia Prepared by Precipitation and Sol−gel methods. *Catal. Today* **2001**, *68*, 21.

(47) Gomez, R.; Lopez, T. Dehydroxylation and the Crystalline Phases in Sol−Gel Zirconia. *J. Sol-Gel Sci. Technol.* **1998**, *11*, 309.

(48) Xie, S.; Iglesia, E.; Bell, A. T. Water-Assisted Tetragonal -to-Monoclinic Phase Transformation of ZrO_2 at Low Temperatures. *Chem. Mater.* **2000**, *12*, 2442.

(49) Mercera, P. D. L.; Van Ommen, J. G.; Doesburg, E. B. M.; Burggraaf, A. J.; Ross, J. R. H. Zirconia as a Support for Catalysts: Evolution of the Texture and Structure on Calcination in Air. *Appl. Catal.* **1990**, *57*, 127.

(50) Mitsuhashi, T.; Ichihara, M.; Tatsuke, U. Characterization and Stabilization of Metastable Tetragonal Zirconium Oxide. *J. Am. Ceram. Soc.* **1974**, *57*, 91.

(51) Garvie, R. C. The Occurrence of Metastable Tetragonal Zirconia as a Crystallite Size Effect. *J. Phys. Chem.* **1965**, *69*, 1238; Stabilization of the Tetragonal Structure in Zirconia Microcrystals. *J. Phys. Chem.* **1978**, *82*, 218.

(52) Mishra, M. K.; Tyagi, B.; Jasra, R. V. Effect of Synthetic Parameters on Structural, Textural and Catalytic Properties of Nanocrystalline Sulfated Zirconia Prepared by Sol−Gel Technique. *Ind. Eng. Chem. Res.* **2003**, *42*, 5727.

Received for review April 25, 2006
Revised manuscript received August 22, 2006
Accepted September 16, 2006

IE060519P